DMD Fast Forward. Published on June 4, 2020 as DOI: 10.1124/dmd.120.000009
This article has not been copyedited and formatted. The final version may differ from this version.

Excretion, Mass balance and Metabolism of [^{14}C] LY3202626 in Humans: An interplay of microbial reduction, reabsorption, and AO oxidation that leads to an extended excretion profile

Kishore Katyayan, Ping Yi[1], Scott Monk, and Kenneth Cassidy

Drug Disposition Eli Lilly and Company, Indianapolis, IN USA;

DMD Fast Forward. Published on June 4, 2020 as DOI: 10.1124/dmd.120.000009
This article has not been copyedited and formatted. The final version may differ from this version.

Running Title: LY3202626 Excretion, Mass Balance and Metabolism in Human

Corresponding author:

Kishore K. Katyayan, Ph. D.

Eli Lilly and Company

Lilly Corporate Center,

Indianapolis IN 46285 U.S.A.

Phone: 317.655.6243

Fax: 317.655.5400

Email: kishore.katyayan@lilly.com

Text pages: 35

Tables: 4

Figures: 10

References: 19

Abstract: 243

Introduction: 457

Discussion: 1637

DMD Fast Forward. Published on June 4, 2020 as DOI: 10.1124/dmd.120.000009
This article has not been copyedited and formatted. The final version may differ from this version.

Abbreviations:

BACE1: β-site amyloid precursor protein-cleaving enzyme 1

AO: Aldehyde Oxidase

AMS: Accelerator Mass Spectrometry

LC-MS: Liquid Chromatography Mass Spectrometry

LC-MS/MS: Liquid Chromatography Tandem Mass Spectrometry

UV: Ultraviolet

Recommended section: Metabolism, Transport, and Pharmacogenomics

DMD Fast Forward. Published on June 4, 2020 as DOI: 10.1124/dmd.120.000009
This article has not been copyedited and formatted. The final version may differ from this version.

Abstract:

The mass balance, excretion, and metabolism of LY3202626 were determined in healthy subjects following oral administration of a single dose of 10 mg (approximately 100 μCi) [^{14}C] LY3202626. Excretion of radioactivity was slow and incomplete, with approximately 75% of the dose recovered after 504 h of sample collection. The mean total recovery of the radioactive dose was 31% and 44% in the feces and urine, respectively. Due to low plasma total radioactivity, plasma metabolite profiling was conducted by accelerator mass spectrometry (AMS). Metabolism of LY3202626 occurred primarily via O-demethylation (M2) and amide hydrolysis (M1, M3, M4, and M5). Overall, parent drug, M1, M2, and M4 were the largest circulating components in plasma, and M2 and M4 were the predominant excretory metabolites. The slow elimination of total radioactivity was proposed to result from an unusual enterohepatic recirculation pathway, involving microbial reduction of metabolite M2 to M16 in the gut, reabsorption of M16, followed by hepatic oxidation of M16 back to M2. Supporting in vitro experiments showed that M2 is reduced to M16 anaerobically in fecal homogenate and M16 is oxidized in the liver by aldehyde oxidase (AO) to M2. LY3202626 also showed a potential to form a reactive sulfenic acid intermediate. A portion of plasma radioactivity was unextractable and presumably bound covalently to plasma proteins. In vitro incubation of LY3202626 in human liver microsomes in the presence of NADPH with dimedone as a trapping agent implicated the formation of the proposed sulfenic acid intermediate.

DMD Fast Forward. Published on June 4, 2020 as DOI: 10.1124/dmd.120.000009
This article has not been copyedited and formatted. The final version may differ from this version.

Significance Statement

The excretion of radioactivity in humans following a single dose 10 mg oral [^{14}C] LY3202626 administration was very slow. The results from in vitro experiments suggested that an interplay between microbial reduction, reabsorption, and AO oxidation (M2 $\rightarrow$ M16 $\rightarrow$ M2) could be reason for extended radioactivity excretion profile. In vitro metabolism also showed that LY3202626 has potential to form a reactive sulfenic acid intermediate that could potentially covalently bind to plasma protein and resulted in unextractable radioactivity from plasma.

DMD Fast Forward. Published on June 4, 2020 as DOI: 10.1124/dmd.120.000009
This article has not been copyedited and formatted. The final version may differ from this version.

Introduction:

Alzheimer's disease is an incurable neurodegenerative disease characterized by a progressive deterioration of cognition and function and is the most common cause of dementia. Accumulation of protein in the brain, specifically extracellular plaques comprised of the beta-amyloid (Aβ) peptide and intracellular neurofibrillary tangles of hyperphosphorylated tau, are believed to be linked to neuronal losses in specific brain regions, giving rise to losses in memory, learning, and cognition. The β-site amyloid precursor protein-cleaving enzyme 1 (BACE1) plays a critical role in the production of Aβ peptides and, consequently, BACE1 inhibitors have been aggressively investigated as potential Alzheimer's therapies. LY3202626, a synthetic small molecule and a potent BACE1 inhibitor, was recently evaluated as a potential treatment for early Alzheimer's disease.

Determination of excretion, mass balance, and metabolism of a drug candidate in humans following a dose of radiolabeled drug is one of most critical steps in drug development (Penner et al., 2009; Roffey et al., 2007). While in vitro and preclinical studies (including ^{14}C preclinical studies) may be helpful in designing early clinical studies, the radioactive clinical study provides the most definite information regarding primary mechanism(s) of clearance, along with the quantitative and comprehensive metabolite profiles in human plasma and excreta. Defining the routes of clearance is crucial for understanding potential inter-individual variability as well as for planning appropriate clinical pharmacology studies, such as drug-drug interaction studies and studies in special populations (renally and hepatically impaired subjects, for example). Characterization of metabolites in this study is important in determining which, if any, metabolites meet regulatory criteria (i.e. metabolites accounting for ≥ 10% of the total circulating drug-related exposure) requiring testing in toxicology studies and evaluation of DDI potential

DMD Fast Forward. Published on June 4, 2020 as DOI: 10.1124/dmd.120.000009
This article has not been copyedited and formatted. The final version may differ from this version.

(FDA, 2020; 2020). The present clinical study was conducted to determine the disposition of radioactivity and LY3202626 in healthy male subjects after oral administration of a pharmacological dose of LY3202626 containing [^{14}C] LY3202626. The total administered dose was 10 mg, which was supported by the available safety data. Data from previous clinical studies indicated that a 10 mg dose was safe and well-tolerated and would result in substantial reductions of plasma and cerebrospinal fluid amyloid β, suggesting a dose in this range would likely be used in subsequent clinical efficacy studies. The radiotracer was administered at approximately 100 μCi to each subject to facilitate characterization of the physiological disposition and metabolism of LY3202626. The quantitative whole-body autoradiography disposition study for LY3202626 in male rats and dosimetry calculations showed that the administration of a single 100 μCi oral dose of [^{14}C] LY3202626 would not be expected to represent a significant radiation exposure risk to healthy human subjects. Results from this study led us to conduct several in vitro metabolism experiments to better understand the disposition and clearance pathways of LY3202626 in humans.

DMD Fast Forward. Published on June 4, 2020 as DOI: 10.1124/dmd.120.000009
This article has not been copyedited and formatted. The final version may differ from this version.

Materials and Methods.

LY3202626, [^{14}C]LY3202626, LSN3200635 (M1), LSN3207841 (M2), LSN3329581 (M4), LSN3226305 (M5), and LSN3420637 (M16) were synthesized by Eli Lilly and Company. For clinical trial use, the investigational drug was supplied as powder in a bottle and was administered as an oral solution in degassed Sprite Zero®. Rat (pooled male Sprague-Dawley, n=10), dog (pooled male Beagle, n=3), monkey (pooled male Cynomolgus, n=3) and human hepatocytes (pooled mixed gender, n=50) and fecal homogenates (pooled male, n=3) were obtained from Bioreclamation/IVT, (Westbury, NY), while human liver cytosol (mixed gender, n=100) were obtained from Xenotech (Lenexa, KS). All other reagents or materials used herein were purchased from Sigma-Aldrich (St. Louis, MO), excluding all cell culture products, which were from Invitrogen Life Technologies (Carlsbad, CA) unless otherwise stated.

Clinical Study Design and Sample Collection

The study was conducted at Covance Clinical Research Unit, Inc in Madison WI, USA in six healthy male subjects between the ages of 27-58 years old (1 Asian, 2 African Americans and 3 Caucasians). The study was conducted in compliance with ethical principles that have their origin in the Declaration of Helsinki and was approved by the institutional review boards at MidLands Independent Review Board (Tampa, FL) and Covance Clinical Research Unit, Inc., (Madison, Wisconsin). After fasting overnight, each of the six subjects received a single oral dose of 10 mg LY3202626 containing approximately 100 μCi [^{14}C]-LY3202626 as an oral solution. Subjects continued to fast up to 4 hours post dose. Whole blood and plasma samples were collected at the following timepoints: 0 (predose), 0.5, 1, 2, 3, 4, 5, 6, 8, 10, 12, 24, 36, 48,

DMD Fast Forward. Published on June 4, 2020 as DOI: 10.1124/dmd.120.000009
This article has not been copyedited and formatted. The final version may differ from this version.

72, 96, 120, 144, and 168 hours postdose, and every 24 hours thereafter until the study discharge criteria had been met. Additional venous blood samples (approximately 15 mL each) were drawn for metabolite profiling predose and at 1, 2, 4, 8, 24, and 48 hours postdose.

Urine samples were collected over the following intervals: before study drug administration (predose), 0 to 6, 6 to 12, 12 to 24, 24 to 48, and 48 to 72 hours postdose, and at 24-hour intervals thereafter until the study discharge criteria had been met. Feces were collected predose and at 24-hour intervals until discharge criteria were met, then mixed with a weighed amount of acetonitrile:water (1:1, v:v) and homogenized. Samples were stored at -20°C until analysis. Samples of expired air were collected for the analysis of $^{14}CO_2$, prior to dosing on Day 1 (negative control sample) and at 2, 4, 8, and 24 hours postdose. Subjects remained at the Clinical Research Unit (CRU) for up to a maximum of 21 days post dose, and were discharged from the CRU at any time after 24 hours urine and fecal samples from two consecutive collections each had radioactivity levels less than 1.0% of the total administered radioactivity in urine and feces combined or Day 22 (21 days postdose). This study was registered at Clinicaltrials.gov with the identifier NCT02555449.

Analysis of Total Radioactivity and LY3202626

Radioactivity in blood, plasma, urine and feces was measured by liquid scintillation counting (LSC) either directly (in urine, plasma, and expired air) or after combustion in an oxidizer apparatus followed by liquid scintillation counting of the trapped $^{14}CO_2$ at Covance Laboratories, Madison, WI. LY3202626 concentrations in plasma were determined with a validated LC-MS/MS assay at Covance Bioanalytical Services, LLC (Indianapolis, Indiana,

DMD Fast Forward. Published on June 4, 2020 as DOI: 10.1124/dmd.120.000009
This article has not been copyedited and formatted. The final version may differ from this version.

USA) using positive ion TurboIon Spray on a Sciex API 3000 mass spectrometer. Details of the assays can be found in Supplemental Materials and Methods.

Metabolite Profiling of Plasma, Urine and Feces

A single plasma AUC pool (Hamilton et al. 1981; Hop et al. 1998) was generated from 0-24 hours after pooling individual timepoints across subjects (0 (predose), 1, 2, 4, 8, and 24 hours). Individual time points of plasma samples at 4, 48, 144, 288, and 504 hours were also pooled across subjects. The AUC pool, and the pooled 4, 144, and 288 hour samples were profiled by HPLC fraction collection with UV in line then offline Accelerator Mass Spectrometry (AMS) (Xceleron, Germantown, Maryland, USA). The pooled 48 and 504 hour plasma were not profiled by HPLC and only "counted" for total radioactivity by AMS. For extraction, initially a protein precipitation procedure was employed. However, due to the poor extraction recovery, the plasma samples were diluted 5 or 10-fold and injected directly onto the HPLC system and fractionated for AMS analysis. Radiochromatograms from the AMS results were generated and LY3202626 and metabolites were expressed as the percentage of region of interest, with the sum of all integrated peaks defined as 100%. Details of the analysis of plasma are shown in Supplemental Materials and Methods.

Metabolite profiling and identification of metabolites in human urine and feces was performed by Eli Lilly and Company. Metabolites in the urine and feces were profiled by high-performance liquid chromatography fraction collection with offline radioactivity counting, and metabolites were identified using LC/MS. Three pooled urine samples (0-24, 24-312, and 480-504 hours) were prepared by pooling the same percentage of urine sample from each collection for individual subject and then pooling across subjects. The pooled urine samples were extracted using Agilent Bond Elut Plexa PCX cartridges (60 mg, 3 mL). Four pooled feces samples (0-24,

DMD Fast Forward. Published on June 4, 2020 as DOI: 10.1124/dmd.120.000009
This article has not been copyedited and formatted. The final version may differ from this version.

24-96, 96-336, and 480-504 hours) were prepared by pooling the same percentage of homogenized feces sample from each collection for individual subject and then pooling across subjects. Pooled fecal samples were extracted first with methanol/acetonitrile (50/50) followed by Agilent Bond Elut Plexa PCX extraction for further clean up. The urine and feces samples were analyzed using radio/HPLC and mass spectrometry. Detailed extraction and analysis methods are provided in the Supplemental Materials and Methods.

LSN3420637 (M16) In Vitro Hepatocytes Incubations

LSN3420637 (M16) was incubated with rat, dog, monkey and human hepatocytes in suspension at 1 million cells/mL with substrate concentration 10 µM with or without 1-aminobenzotriazole (ABT) (1 mM) or hydralazine (200 µM) at 37°C for 4 hours. An equal volume of acetonitrile was added to quench the reaction at the end of incubation. The samples were centrifuged and the supernatants were analyzed by a UHPLC system using a waters Acquity BEH C18, 2.1 x 10 cm (1.7 µm particle size) and following LC condition: Mobile phase A (water containing 0.2% formic acid), Mobile phase B: (Acetonitrile), Flow rate: 0.5 mL/min, Gradient (min/B%): 0/5, 0.4/5, 3.5/50, 5/90, 6/90, 6.1/5, 8/stop. Accurate mass LC/MS, LC/MS/MS (Thermo OrbiTrap Velos mass spectrometer fitted with Heated Electrospray Ionization (HESI), Thermo Fisher Scientific with positive ion detection (HESI) were used for parent and metabolite identification (Spray voltage = 4.5 kV, Capillary temperature = 300°C, Source heater temperature = 350°C, sheath gas = 60, auxiliary gas = 20, sweep gas = 20, collision energy (HCD) = 35).

DMD Fast Forward. Published on June 4, 2020 as DOI: 10.1124/dmd.120.000009
This article has not been copyedited and formatted. The final version may differ from this version.

LSN3420637 (M16) Incubation in Human Liver Cytosol and M2 isolation

LSN3420637 was incubated with human liver cytosol at 1 mg/mL protein with substrate concentration 50 µM at 37°C for 4 hours. The total volume of incubation was approximately 80 mL. An equal volume of acetonitrile was added to quench the reaction at the end of incubation. The samples were centrifuged and the supernatant was concentrated to approximately 20 mL in GeneVac (a vacuum centrifugal evaporator) for M2 isolation.

M2 isolation was conducted by a semi-preparative HPLC system using a 25 x 10 mm C18 HPLC column (5 µm particle size) and following LC condition: Mobile phase A (0.2% formic acid), Mobile phase B: (Acetonitrile/methanol (25/75)), Flow rate: 6 mL/min, Gradient (min/B%): 0/20, 5/20, 20/50, 21/90, 30/90, 30.1/20, 55/stop. Fractions were collected at 15 second intervals. Selected fractions were analyzed by LC/MS. Fractions containing high purity of M2 were combined, freeze-dried and submitted for NMR analysis.

LSN3207841 (M2) incubation with Human Fecal Microflora

The fecal homogenates were purchased from Bioreclamation, Inc (New York, USA). Fresh feces were collected from 3 healthy subjects individually. Upon collection, feces was mixed with 10% glycerol in 100 mM sodium phosphate buffer (pH 7.4) (1:4, w:v) and homogenized. The homogenates were stored at -70°C until use. Fecal homogenates pooled from the 3 subjects were used for this experiment. To deactivate fecal bacteria, an aliquot of fecal homogenate was placed in 100°C water bath for 1 hour. The heated and non-heated fecal homogenates were inoculated in BHI (Brain Heart Infusion) medium (Remel, Inc.) containing 10 µM test compound and incubated under anaerobic atmosphere for 1 week in a desiccator at 37ºC.

DMD Fast Forward. Published on June 4, 2020 as DOI: 10.1124/dmd.120.000009
This article has not been copyedited and formatted. The final version may differ from this version.

The anaerobic atmosphere in the desiccator was created by placing two AnaeroGen paper sachets (Oxoid, Ld.) into the desiccator. An anaerobic indicator pill was also placed in the desiccator to monitor anaerobic status. After 1 week incubation, samples were extracted with acetonitrile and analyzed by LC-MS as described above.

NMR Identification of M2 from In Vitro Incubation of M16

NMR identification of M2 was performed on Bruker 600 AVANCE III HD (Bruker BioSpin Corporation, San Jose, CA) instruments with field strengths of 14.1 T with CP QCI 600S3 H/F-C/N-D-05 Z probe. All analytes were dissolved in CD_3OD, and the experiments were conducted at 25°C. Standard proton spectra were used to confirm the structure of the metabolite. Spectra were referenced with respect to water signal at 3.31ppm for ^1H.

LY3202626 Incubation with Human Liver Microsomes and Dimedone

LY3202626 (1 μM) was incubated with human liver microsomes at 1 mg/mL, 2 mM dimedone and 2 mM NADPH in total volume of 1 mL (100 mM Phosphate buffer, pH 7.4) for 45 min at 37°C in a shaking water bath. The reaction was stopped by 2 mL of acetonitrile then centrifuged for approximately 10 min at 4000 RPM, and samples were analyzed by a HPLC system using a waters Acquity BEH C18, 2.1 x 100 mm (1.7 μm particle size) and following LC condition: Mobile phase A (water containing 0.2% formic acid), Mobile phase B: (Acetonitrile), Flow rate: 0.5 mL/min, Gradient (min/B%): 0/5, 0.4/5, 3.5/50, 4/90, 4.25/90, 4.5/5, 6/stop. Accurate mass LC/MS, LC/MS/MS (Waters Synapt G2-S) were used for parent

DMD Fast Forward. Published on June 4, 2020 as DOI: 10.1124/dmd.120.000009
This article has not been copyedited and formatted. The final version may differ from this version.

compound and dimedone adduct identification (ESI positive, Capillary = 1.0 kV, Sample cone = 40 V, Source temperature = 120°C, Desolvation = 500°C, and collision energy = 10-35 V).

In Vitro Assessment of Permeability of LSN3420637 (M16) and LSN3207841 (M2)

MDCK cells transfected with MDR1 (ABCB1) obtained at passage number 12 from P. Borst at The Netherlands Cancer Institute (Amsterdam, The Netherlands) were used for apical-to-basolateral (A-B) and basolateral-to-apical (B-A) flux determination of LSN3420637 (M16) and LSN3207841 (M2). Details of the method and analysis are provided in the Supplemental Materials and Methods.

Pharmacokinetic Analysis

Pharmacokinetic parameter estimates of total radioactivity (in blood and plasma) and LY3202626 (in plasma) were calculated by standard noncompartmental methods of analysis using Phoenix WinNonlin Version 6.2.1. The primary PK parameters calculated included maximum observed drug concentration (C_{max}), time of maximum observed drug concentration (t_{max}), area under the concentration versus time curve (AUC) from time zero to time t, where t was the last time point with a measurable concentration ($AUC_{[0\text{-}t_{last}]}$), AUC from zero to infinity ($AUC_{[0\text{-}\infty]}$), percentage of $AUC_{(0\text{-}\infty)}$ extrapolated ($\%AUC_{[t_{last}\text{-}\infty]}$), and half-life associated with the terminal rate constant in noncompartmental analysis ($t_{1/2}$). For LY3202626 in plasma, additional noncompartmental parameters including apparent total body clearance of drug after extravascular administration (CL/F), apparent volume of distribution during the terminal phase after extravascular administration (V_z/F), and apparent volume of distribution at steady state after extravascular administration (V_{ss}/F), were calculated.

DMD Fast Forward. Published on June 4, 2020 as DOI: 10.1124/dmd.120.000009
This article has not been copyedited and formatted. The final version may differ from this version.

DMD Fast Forward. Published on June 4, 2020 as DOI: 10.1124/dmd.120.000009
This article has not been copyedited and formatted. The final version may differ from this version.

Results:

Human Pharmacokinetics, Excretion and Metabolism

The mean plasma concentration versus time for LY3202626 in plasma and total radioactivity in both plasma and whole blood following a single 10-mg dose of LY3202626 containing approximately 100 μCi of [^{14}C]-LY320262 are shown in Figure 1. The PK parameters for plasma LY3202626, plasma total radioactivity, and whole blood total radioactivity are presented in Table 1. Radioactivity was quantifiable in plasma up to 96 hours by LSC and up to 504 hours by Accelerator Mass Spectrometry (AMS). The median t_{max} for LY3202626 in plasma was 4.00 hours postdose, with secondary peaks generally observed at approximately 10 hours and again at 24 to 36 hours postdose. The mean $t_{1/2}$ of plasma LY3202626 was 24.5 hours, with values for individual subjects ranging from 17.0 to 52.2 hours. The last quantifiable time point for LY3202626 in individual subjects ranged from 96 hours postdose (Subject 1006) to 336 hours postdose (Subject 1002). The median t_{max} values for total radioactivity in plasma and whole blood were 3.50 hours and 4.00 hours postdose, respectively, which is similar to that for plasma LY3202626. Secondary peaks were generally observed for total radioactivity at approximately 10 hours postdose and again at 24 to 36 hours. The mean $t_{1/2}$ of plasma total radioactivity was 32.5 hours. A $t_{1/2}$ could not be calculated for total radioactivity in whole blood due to the poorly-defined terminal phase. The whole blood to plasma total radioactivity ratios ranged from 0.650 to 0.806 through 10 hours postdose (data not shown). Exposure to LY3202626 accounted for approximately 32% and 42% of total plasma radioactivity based on $AUC_{(0-48)}$ and C_{max}, respectively, indicating the presence of one or more circulating metabolites.

DMD Fast Forward. Published on June 4, 2020 as DOI: 10.1124/dmd.120.000009
This article has not been copyedited and formatted. The final version may differ from this version.

Excretion and mass balance in urine and feces

The cumulative excretion of total radioactivity up to 504 hours postdose is depicted graphically in Figure 2. The overall mean (± SD) recovery of radioactivity in urine and fecal samples was 75.4% (± 4.84%) over the 504-hour study, with recovery in individual subjects ranging from 68.8% to 81.5%. A mean (± SD) of 44.2% (± 3.70%) of the dose was excreted in urine and 31.3% (± 4.24%) was excreted in feces through the last collection interval. Total radioactivity was excreted slowly, and the majority was recovered in the first 264 hours postdose (approximately 65.6%). The maximum mean amounts of [^{14}C]-LY3202626-derived radioactivity were observed in samples collected from 0 to 6 hours postdose for urine (8.50% of the dose) and from 72 to 96 hours postdose in feces (4.72% of the dose). Levels of radioactivity observed in expired air samples were very low (near the limit of quantitation). Therefore, the percent of dose in expired air was not calculated.

Radioprofiling and metabolite identification

Radioprofiling of the 0-24 hour AUC plasma pool by AMS showed that parent was the largest peak, accounting for 38.0% of the total radioactivity (Table 2, Figure 3). Identified metabolites included M1 (the aniline from the amide hydrolysis, LSN3200635), M2 (O-desmethyl, LSN3207841), M3 (the carboxylic acid from the amide hydrolysis, LSN3170994), M4 (glycine conjugate of M3), M5 (N-acetyl conjugate of M1, LSN3226305) and M16 (M2 - O, M2 reduction, LSN3420637), accounting for 2.27%, 4.41%, 3.86%, 11.90% , <1% and <1% of the total radioactivity, respectively. Due to poor extraction recoveries (<70%), diluted plasma

DMD Fast Forward. Published on June 4, 2020 as DOI: 10.1124/dmd.120.000009
This article has not been copyedited and formatted. The final version may differ from this version.

samples were directly injected onto HPLC column for radioprofiling by AMS. Metabolite identification in plasma was achieved by matching UV traces of synthetic standards spiked in plasma to radioactive peaks. Radioactivity that eluted during column wash (HPLC retention time around 100 min) (Region A) accounted for 33.5% of the total radioactivity. Pooled plasma samples at 4, 144, and 288 hours were also profiled by AMS. At 4 hours, parent was the largest peak (43.4% of the total radioactivity), and M4 was the most abundant metabolite (10.3% of the total radioactivity). Over time, the relative percentages for M3, M4, and parent decreased while M1, M2, and M16 increased, suggesting rapid elimination of M3, M4, and parent, and slow elimination and/or formation of M1, M2, and M16. The relative percent of sample radioactivity for Region A increased over time, from 30% at 4 hours to 54% at 288 hours. Following extraction of plasma using acetonitrile and methanol (protein precipitation), the percent of unextracted radioactivity (remaining in protein pellet) matched very well with that in Region A in all plasma samples injected directly to AMS (4 hour, 144 hour, 288 hour, and 0-24 hour AUC pool). These results suggest that Region A might be LY3202626 or metabolites associated with protein-related material(s).

Urine samples collected from 0-24, 24-312, and 480-504 hour were pooled across subjects and profiled. Parent drug, M1, M2, M4, M5, and M21 (having the same molecular ion and similar MSMS fragments as parent drug) were identified and quantified in urine (Table 3, Figure 4, and Supplemental Table S1). Parent drug accounted for approximately 2% of the dose in the urine samples analyzed. M2 and M4 were the two most abundant urinary metabolites, accounting for 9% and 21% of the dose, respectively, in the urine samples analyzed. In the early collection period (0-24 hours), M4 was the predominant radioactive peak accounting for 73% of the total radioactivity in sample (Figure 4). Over time, percentage of radioactivity attributed to

DMD Fast Forward. Published on June 4, 2020 as DOI: 10.1124/dmd.120.000009
This article has not been copyedited and formatted. The final version may differ from this version.

M4 decreased (39% in 24-312 hour, and 0% in 480-504 hour urine). In contrast, the relative percent radioactivity of M2 compared to total radioactivity increased over time, accounting for 7%, 32%, and 76% of the total radioactivity in 0-24, 24-312, and 480-504 hour urine samples, respectively. These data suggested relatively rapid excretion for M4, and slow excretion and/or formation for M2. Metabolites M1, M5, and M21, also identified in urine, each accounted for less than 2% of the dose.

Fecal samples collected from 0-24, 24-96, 96-336, and 480-504 hour were pooled across subjects and profiled. Parent drug, M2, M5, M16, and M21 were identified and quantified in feces (Table 3, Figure 5 and Supplemental Table S1). Parent drug accounted for 2% of the dose in the feces analyzed. M2 and M16 were the two most abundant fecal metabolites across all the collection time periods, accounting for approximately 11% and approximately 7% of the dose, respectively, in the feces analyzed. M5 and M21 individually accounted for less than 2% of the dose in the feces analyzed. In the 480-504 hour feces, M2 and M16 were the only radioactive peaks observed.

In vitro Incubations:

A small percentage of plasma radioactivity (Region A) could not be extracted and the relative percent this unextractable radioactivity increased over time of plasma collection (Table 2). The percent of unextracted radioactivity (remaining in protein pellet) matched very well with that in Region A in various plasma samples, suggesting that Region A might be LY3202626 or metabolites associated with protein-related material(s). It is known that some sulfur-containing drugs may form reactive sulfenic acid species that in turn can react with nucleophilic moieties of

DMD Fast Forward. Published on June 4, 2020 as DOI: 10.1124/dmd.120.000009
This article has not been copyedited and formatted. The final version may differ from this version.

proteins (Mansuy and Dansette, 2011). Dimedone has been quite successfully used as a trapping agent to capture sulfenic acid species formed by metabolic activation in vitro (Gupta et al., 2016a, 2016b). To assess the possible formation of a reactive sulfenic acid metabolite, LY3202626 was incubated in human liver microsomes in the presence of dimedone and in the presence and absence of NADPH. LY3202626-dimedone adducts were observed in the presence of NADPH but not in the absence of NADPH (Figure 6).

In order to investigate potential for reduction of M2 to M16 in the gut, an incubation of M2 with human fecal microflora under anaerobic atmosphere was conducted. The results showed the reduction of M2 to M16 in human fecal microflora under anaerobic atmosphere, but no such reduction was observed in medium control or with heat deactivated fecal microflora (Figure 7). The permeability of M2 and M16 was also evaluated by studying transport across MDCK-MDR1 monolayers. Results showed M2 as a highly-efficient P-gp substrate with very slow passive permeability, while M16 is a moderate P-gp substrate with very fast passive permeability and fast permeability even against the active efflux pump (160 nm/s) (Table 4).

To investigate the potential for the oxidation of M16 to M2, M16 (LSN3420637) was incubated in rat, dog, monkey, and human hepatocytes. The results showed the formation of M2 in rat, monkey, and human hepatocytes, but not in dog hepatocytes. M2 formation from M16 was inhibited by hydralazine (an aldehyde oxidase inhibitor; Sun Q et al, 2011; Strelevitz et al., 2012) but not by 1-aminobenzotriazole (ABT) (a pan-CYP inhibitor, Ortiz de Montellano and Mathews, 1981; Johnson et al, 1985; Williams et al., 2003) (Supplement Table S2). M16 incubations in hepatocytes also showed the formation of another hydroxy metabolite M1 in all the species, which was not inhibited by ABT or hydralazine. Figure 8 shows the extracted ion chromatograms from these incubations in human hepatocytes. To confirm the position of the

DMD Fast Forward. Published on June 4, 2020 as DOI: 10.1124/dmd.120.000009
This article has not been copyedited and formatted. The final version may differ from this version.

oxidation of M2 generated from M16 in vitro, M16 was incubated in human liver cytosol and M2 was isolated from the incubation and analyzed by NMR. The NMR result confirmed that M2 generated from M16 is LSN3420637 (data not shown). It should be noted that the concentration of hydralazine used in these incubations was high (i. e. 200 μM), which could possibly inhibit some of the CYP enzymes (Ying et. al, 2019). However, lack of the formation of M2 by dog hepatocytes, no inhibition of the formation of M2 in the presence of ABT, and the isolation of M2 using human cytosols provide additional support that the M2 is formed by aldehyde oxidase (AO) and not CYP enzymes.

DMD Fast Forward. Published on June 4, 2020 as DOI: 10.1124/dmd.120.000009
This article has not been copyedited and formatted. The final version may differ from this version.

Discussion

In this study, [^{14}C] LY3202626 was administered orally at a pharmacologically relevant dose of 10 mg [100 µCi] to six healthy male volunteers (https://clinicaltrials.gov/ct2/show/NCT02555449). After collection of excreta for up to the maximum of 21 days only 74.5 % (31.4% urine and 44% feces) of the dose was recovered in urine and feces with no appreciable amount of radioactivity obtained in expired air.

Although there is no formal cut off for "acceptable" recovery in a human ADME study, the overall recovery from this study falls well within the data reported by Roffey et. al (2007). The overall recovery from this study was sufficient to meet the objectives of the study, which included understanding the major clearance pathways as well as identification of the major metabolites. The pharmacokinetics of LY3202626 and total radioactivity also showed unusual characteristics, with secondary peaks observed in the PK profiles of LY3202626 (plasma) and total radioactivity (blood and plasma) following the C_{max} peaks at 4.0, 3.5 and 4.0 hours, respectively. The secondary peaks for LY3202626 and for total radioactivity appeared between 10 and 36 hours post dose. A metabolite (M21, Figure 9) whose structure could not be determined has the same molecular and product ion as parent, suggesting it could be a Phase II conjugate that is unstable when ionized in the mass spectrometer, undergoing source-induced fragmentation. It is possible that such a labile Phase II conjugate could be hydrolyzed in the intestine followed by reabsorption, leading to the secondary peaks observed for LY3202626 and total radioactivity. Exposure to LY3202626 accounted for approximately 32% and 42% of total plasma radioactivity based on $AUC_{(0-48)}$ and C_{max}, respectively, indicating the presence of one or more circulating metabolites. Overall, parent drug, M1, M2, M3 and M4 were the predominant circulating components in plasma, and M2 and M4 were the predominant excretory metabolites.

DMD Fast Forward. Published on June 4, 2020 as DOI: 10.1124/dmd.120.000009
This article has not been copyedited and formatted. The final version may differ from this version.

Parent drug and M4 were the only components in plasma that accounted for >10% of radioactivity in the AUC_{0-24}. Over time, the relative percentages for M3, M4, and parent decreased in plasma while M1, M2, and M16 increased, suggesting rapid elimination of M3, M4, and parent, and slower elimination and/or formation of M1, M2, and M16.

LY3202626 was well absorbed and extensively metabolized in healthy subjects following a single oral dose of 10 mg [^{14}C]-LY3202626, with only 4% of dose excreted as parent drug in urine and feces. In urine, parent drug accounted for approximately 2% of the dose and metabolites M2 and M4 were the two most abundant urinary metabolites, accounting for 9% and 21% of the dose, respectively. In feces, parent drug accounted for 2% of the dose and metabolite M2 and M16, the two most abundant fecal metabolites, accounting for approximately 11% and 7% of the dose, respectively. Overall, the data from the study demonstrates that metabolism is the major route of clearance for LY3202626, and metabolism of LY3202626 occurs primarily through O-demethylation (M2) and amide hydrolysis (M1, M3, M4, and M5). Figure 9 shows proposed metabolism pathways of LY3202626 in humans.

As previously discussed, the mass balance excretion results from this study appeared less than optimal and were somewhat unanticipated. In preclinical ^{14}C ADME studies conducted prior to the human ADME study, the recovery of radioactive dose was almost 100% by 168 hr in rats and >90% by 192 hr in dogs (Supplement Figure S1). Furthermore, radioactivity was eliminated rapidly, with approximately 97% of the total radioactive dose eliminated in the first 48 hours postdose following a single oral administration in rat and approximately 84% of the dose eliminated in the first 72 hours postdose following a single oral administration in dog. Particularly slow excretion of radioactivity both in urine and feces in humans, as well as slow clearance of some of the metabolites (M1, M2 and M16) from plasma, was puzzling.

DMD Fast Forward. Published on June 4, 2020 as DOI: 10.1124/dmd.120.000009
This article has not been copyedited and formatted. The final version may differ from this version.

Furthermore, a percentage of plasma radioactivity could not be extracted (Region A), and this unextractable region represented a greater percent of radioactivity in plasma samples at later time points. In contrast, the percentage of plasma radioactivity recovery was almost complete in rat and dog (86-94% for rat and 95-100% for dog; Supplemental Table 3A and 3B). The amount of radioactivity found in the human plasma protein pellet (when re-suspended using acetonitrile and methanol), matched the amount of radioactivity represented by Region A at various time points after direct injection of diluted plasma, and these data suggest that Region A might be LY3202626 and/or metabolites associated with protein-related material(s). Sulfur-containing drugs are known to possibly form reactive sulfenic acid species that in turn may react with nucleophilic (sulfhydryl) moieties of proteins (Mansuy and Dansette, 2011). The observation of a LY3202626-dimedone adduct formed in human liver microsome incubations containing NADPH and dimedone (Figure 6) supports the hypothesis that the unextractable portion of radioactivity in plasma could be due to one or more adducts formed by a sulfenic acid metabolic intermediate of LY3202626 reacting with plasma protein to form a covalent adduct.

Metabolite M4 was the predominant radioactive peak in the 0-24 hour urine sample, but it was not quantifiable in the 480-504 hour sample (Figure 4). In contrast, the relative percent radioactivity of M2 increased over time. In feces, M2 and M16 were the two most abundant fecal metabolites across all the collection time periods (Figure 5). In fact, M2 and M16 were the only radioactive peaks observed in the 480-504 hour feces. Based upon slow excretion of radioactivity, the presence of M2 as the most prominent metabolite peak at later time points in urine, and the presence of M2 and M16 as the two most abundant fecal metabolites at all the collection time periods, it was hypothesized that the slow excretion of radioactivity in excreta could be due to reduction/oxidation cycling between M2 and M16. To investigate this

DMD Fast Forward. Published on June 4, 2020 as DOI: 10.1124/dmd.120.000009
This article has not been copyedited and formatted. The final version may differ from this version.

possibility, several in vitro experiments were conducted. Formation of M2 from M16 in rat, monkey, and human hepatocytes, but not in dog hepatocytes, and inhibition of the formation of M2 from M16 in the presence of hydralazine but not in the presence of ABT, suggested that metabolism of M16 to M2 is mediated by AO. To confirm that M2 was formed via AO from M16, metabolite M16 was incubated in human cytosol and M2 was isolated and purified. The NMR spectra obtained from the cytosol incubation matched M2 (data not shown). Incubation of metabolite M2 with human feces under an anaerobic atmosphere showed that M2 is reduced to M16 by gut microflora. In addition, an in vitro permeability assessment showed M2 is a highly-efficient P-gp substrate with very slow passive permeability. In contrast, M16 was found to be a moderate P-gp substrate with very fast passive permeability (Table 4). Based up on these results, we propose that LY3202626 is first converted to M2 by CYP demethylation, which gets excreted into intestine, where its very low permeability and P-gp substrate recognition prevents reabsorption. Metabolite M2 is then anaerobically reduced to M16 by gut microflora, and the resulting highly-permeable M16 is reabsorbed. After reabsorption, metabolite M16 is oxidized back to M2 in the liver by AO or hydrolyzed to M1 as illustrated in Figure 10. Such enterohepatic recirculation might contribute to extended retention of M1, M2, and M16. The reduction/oxidation reactions form a complete enterohepatic cycling process. The lack of an extended excretion profile of radioactivity due to M2/M16 enterohepatic re-circulation in preclinical species administered [^{14}C]LY3202626 could be due to the minimal formation of M2 in rat and inherit lack of AO activity in dog (Supplement Table S4). Li et. al, (2012) reported a similar reduction and oxidation of BILR 355 (an inhibitor of the human immunodeficiency virus) by gut bacteria and AO, respectively. In that particular study, ritonavir was used to inhibit the CYP3A-mediated metabolism of BILR 355 and to increase the clinical exposure of BILR 355.

DMD Fast Forward. Published on June 4, 2020 as DOI: 10.1124/dmd.120.000009
This article has not been copyedited and formatted. The final version may differ from this version.

However, the inhibition not only increased the levels of BILR 355, but a metabolite (BILR 516) that was not detected previously in humans dosed with BILR 355 alone was found. Subsequent in vitro studies revealed that a metabolic switching of BILR 355 occurs in the presence of ritonavir. BILR 355 is reduced to an intermediate, BILR 402, by gut bacteria, and the reduced metabolite (BILR 402) is then oxidized by aldehyde oxidase to form BILR 516, the disproportionate human metabolite. Ross et al. (1988) similarly reported that 5-(4-acetamidopheyl)pyrazine-2(1H)-one, containing a pyrazinone moiety, a structure similar to the hydroxy pyrazine in M2, undergoes reduction of the pyrazinone to the corresponding pyrazine metabolite by microflora in gut. The authors speculated that the pyrazine metabolite might be re-absorbed from gut and subsequently oxidized in liver to an N-oxide.

In conclusion, following a single 10 mg [^{14}C] LY3202626 oral dose administration to humans, overall recovery of radioactivity even after three weeks of collection was only 75%, which falls well within the data reported by Roffey et. al (2007). The overall recovery from this study was sufficient to meet the objectives of the study, which included understanding the major clearance pathways as well as identification of the major metabolites. Several in vitro experiments carried out with LY3202626 provided strong support for the proposed mechanisms leading to the long retention of radioactivity in circulation and excreta as illustrated in Figure 10. Similar observations of enterohepatic re-circulation have also been made previously (Ross et al. 1988, Li et al 2012). Another important observation from the study was a portion of plasma radioactivity was unextractable. Observation of a dimedone adduct following in vitro incubation of LY322626 with liver microsome and dimedone suggests that the unextracted plasma radioactivity could be due to formation of plasma protein adducts by reactive sulfenic acid metabolite intermediates of LY3202626. Considering a proposed therapeutic dose of 10 mg, the body burden due to

DMD Fast Forward. Published on June 4, 2020 as DOI: 10.1124/dmd.120.000009
This article has not been copyedited and formatted. The final version may differ from this version.

formation of such a reactive intermediate would have been expected to be low (Lammert et al, 2008; Stepan et la., 2011). However, as further development of this compound was halted, any impact of such a reactive intermediate in human will be unknown.

Acknowledgments;

Authors would like to acknowledge Jeffrey Alberts and Geri Sawada for performing dimedone trapping assays and permeability assays, respectively.

DMD Fast Forward. Published on June 4, 2020 as DOI: 10.1124/dmd.120.000009
This article has not been copyedited and formatted. The final version may differ from this version.

Authorship Contributions

Participated in research design: Katyayan, Yi, Monk, and Cassidy

Conducted experiments: Yi

Contributed new reagents or analytic tools: Katyayan, Yi, and Cassidy

Performed data analysis: Katyayan, Yi, and Cassidy

Wrote or contributed to the writing of the manuscript: Katyayan, Monk, and Cassidy

DMD Fast Forward. Published on June 4, 2020 as DOI: 10.1124/dmd.120.000009
This article has not been copyedited and formatted. The final version may differ from this version.

References:

FDA (2020) Guidance for Industry: Safety Testing of Drug Metabolites, Version 2, US Department of Health and Human Services FDA, Center for Drug Evaluation and Research, Silver Spring, MD.

FDA (2020) In Vitro Drug Interaction Studies — Cytochrome P450 Enzyme- and Transporter-Mediated Drug Interactions Guidance for Industry, US Department of Health and Human Services FDA, Center for Drug Evaluation and Research, Silver Spring, MD.

Gupta V, and Carroll KS (2016a) Profiling the reactivity of cyclic *C*-nucleophiles towards electrophilic sulfur in cysteine sulfenic acid. Chem Sci 7: 400–415.

Gupta V, Paritala H, Carroll KS (2016b) Reactivity, selectivity and stability in sulfenic acid detection: A comparative study of nucleophilic and electrophilic probes. Bioconjug Chem 27: 1411–1418.

Hamilton R, Garnett WR, and Kline BJ (1981) Determination of Mean Valproic Acid Serum Level by Assay of a Single Pooled Sample. Clin Pharmacol Ther 29: 408-413.

Hop CECA, Wang Z, Chen Q, and Kwei G (1998) Plasma Pooling Methods to Increase Throughput for In Vivo Pharmacokinetic Screening. J Pharm Sciences 87: 901-903.

Johnson C, Stubley-Beedham C, Stell JG (1985) Hydralazine: a potent inhibitor of aldehyde oxidase activity in vitro and in vivo. Biochem Pharmacol 34: 4251–4256.

Lammert C, Einarsson S, Saha C, Niklasson A, Bjornsson E, Chalasani N (2008) Relationship between daily dose of oral medications and idiosyncratic drug-induced liver injury: search for signals. Hepatology 47: 2003-2009.

Li Y, Xu J, Lai WG, Whitcher-Johnstone A, Tweedie DJ (2012) Metabolic switching of BILR 355 in the presence of ritonavir. II. Uncovering novel contributions by gut bacteria and aldehyde oxidase. Drug Metab Dispos 40: 1130-1137.

Mansuy D and Dansette PM (2011) Sulfenic acids as reactive intermediates in xenobiotic metabolism. Arch Biochem Biophys 507: 174–185.

Ortiz de Montellano PR and Mathews JM (1981) Autocatalytic alkylation of the cytochrome P-450 prosthetic haem group by 1-aminobenzotriazole. Isolation of an N N-bridged benzyneprotoporphyrin IX adduct. Biochem J 195: 761–764.

Penner N, Klunk LJ, Prakash C (2009) Human radiolabeled mass balance studies: objectives, utilities and limitations. Biopharm Drug Dispos 30: 185–203.

Roffey SJ, Obach RS, Gedge JI, Smith DA (2007) What is the objective of the mass balance study? A retrospective analysis of data in animal and human excretion studies employing radiolabeled drugs. Drug Metab Rev 39:17–43.

Ross DA, Osborne PM, Pue MA, Blake TJ, Chenery RJ, and Metcalf R (19880 The metabolism of 5-(4-acetamidopheyl)pyrazine-2(1H)-one in rat, dog and cynomolgus monkey. Xenobiotica 18:1373-1387.

Stepan AF, Walker DP, Bauman J, Price DA, Baillie TA, Kalgutkar AS, Aleo MD (2011) Structural alert/reactive metabolite concept as applied in medicinal chemistry to mitigate the risk of idiosyncratic drug toxicity: a perspective based on the critical examination of trends in the top 200 drugs marketed in the United States. Chem Res Toxicol 24:1345-1410.

Strelevitz TJ, Orozco CC, Obach RS (2012) Hydralazine as a selective probe inactivator of aldehyde oxidase in human hepatocytes: estimation of the contribution of aldehyde oxidase to metabolic clearance. Drug Metab Dispos 40:1441-8.

Sun Q, Harper TW, Dierks EA, Zhang L, Chang S, Rodrigues AD, Marathe P. (2011) 1-Aminobenzotriazole, a known cytochrome P450 inhibitor, is a substrate and inhibitor of N-acetyltransferase. Drug Metab Dispos 39:1674-1679.

Williams JA, Hurst SI, Bauman J, Jones BC, Hyland R, Gibbs JP, Obach RS, and Ball SE (2003) Reaction phenotyping in drug discovery: moving forward with confidence? Curr Drug Metab 4:527–534.

Yang X, Johnson N, Di L (2019) Evaluation of Cytochrome P450 Selectivity for Hydralazine as an Aldehyde Oxidase Inhibitor for Reaction Phenotyping. J Pharm Sci 108:1627-1630.

DMD Fast Forward. Published on June 4, 2020 as DOI: 10.1124/dmd.120.000009
This article has not been copyedited and formatted. The final version may differ from this version.

Footnotes.

a) financial support: This work was supported by Eli Lilly and Company.

b) The work was presented at International Society for the Study of Xenobiotics, 2019 as a poster.

c) Reprint requests. Kishore K. Katyayan, Ph. D., Eli Lilly and Company, Lilly Corporate Center, Indianapolis IN 46285 U.S.A., Email: kishore.katyayan@lilly.com

[1]Current affiliation: Covance, Madison, WI USA

DMD Fast Forward. Published on June 4, 2020 as DOI: 10.1124/dmd.120.000009
This article has not been copyedited and formatted. The final version may differ from this version.

Figure Caption.

Figure 1: Mean (± SD) concentrations of radioactivity in blood and plasma and mean (± SD) concentrations of parent compound (LY3202626) following oral administration of a single 10-mg (100 µCi) oral dose of [^{14}C] LY3202626 to healthy subjects.

Figure 2: Mean (+SD) cumulative percent of radioactive dose recovered in urine and feces at specified intervals following oral administration of a single 10-mg (100 µCi) oral dose of [^{14}C] LY3202626 to healthy subjects.

Figure 3: UV chromatogram (250 nm) generated from injection of diluted plasma spiked with synthetic standards of M1, M2, M3, M4, M5, M16, and P (parent) overlaid against a ^{14}C radiochromatogram based on the AMS detection of fractions and fraction pools collected from direct injection of 0-24 hour AUC pool plasma following oral administration of a single 10-mg (100 µCi) oral dose of [^{14}C] LY3202626 to healthy subjects. Note that UV trace of the parent (P) is obscured by its radioactive trace.

Figure 4: Reconstructed radioprofiles of urines following oral administration of a single 10-mg (100 µCi) oral dose of [^{14}C] LY3202626 to healthy subjects.

Figure 5: Reconstructed radioprofiles of feces following oral administration of a single 10-mg (100 µCi) oral dose of [^{14}C] LY3202626 to healthy subjects.

Figure 6A: Extracted ion chromatograms of LY3202626 and its dimedone adduct following incubation of LY3202626 in human liver microsomes in the absence (A) and presence of NADPH (B).

DMD Fast Forward. Published on June 4, 2020 as DOI: 10.1124/dmd.120.000009
This article has not been copyedited and formatted. The final version may differ from this version.

Figure 6B: The proposed metabolic for the formation of LY3202626-dimedone adduct following incubation of LY32026 in human liver microsome incubations in the presence of NADPH and dimedone.

Figure 7: Extracted ion chromatograms of M2 (LSN3207841) and incubations under anaerobic condition for 168 hours with BHI medium (A), with deactivated human fecal microflora (B), and non- deactivated human fecal microflora (C).

Figure 8: Extracted ion chromatograms of M16 (LSN3420637) incubations in human hepatocytes for 4 hours in the absence of any inhibitor (A), in the presence of ABT (B) and in the presence of hydralazine (C).

Figure 9: The proposed metabolic scheme for LY3202626 following a single oral dose of 10 mg

[^{14}C]-LY3202626 to healthy humans. This test article is dual radiolabeled and the dosing included 1:1 mix of both labeled compounds, * signifies the positions of the radiolabel. F, P, and U indicate presence in feces, plasma and urine, respectively.

Figure 10: Hypothesis illustrating enterohepatic recirculation of radioactive material and possible cause of slow excretion of radioactivity, involving microbial reduction of metabolite M2 to M16 in the gut, reabsorption of M16 and followed by hepatic oxidation of M16 back to M2.

Table 1: Summary of Pharmacokinetic Parameter Estimates of LY3202626 in Plasma and Total Radioactivity in Plasma and Whole Blood following Oral Administration of a Single 10-mg Dose of [^{14}C] LY3202626

PK Parameters	Geometric Mean (CV%)		
	Plasma LY3202626 (N=6)	Plasma total radioactivity[a] (N=6)	Whole blood total radioactivity[a] (N=6)
AUC(0-t_{last}) (ng·h/mL)	294 (48)	814 (31)	240 (60)
AUC(0-∞) (ng·h/mL)	298 (47)	1120 (27)	NC
%AUC(t_{last}-∞)	1.19 (48)	27.0 (19)	NC
AUC$_{(0-10)}$ (ng·h/mL)	70.0 (36)	207 (14)	146 (17)
AUC$_{(0-48)}$ (ng·h/mL)	227 (37)	711 (15)	NC
C_{max} (ng/mL)	10.7 (32)	25.2 (16)	21.0 (18)
t_{max}[b] (h)	4.00 (2.00 – 10.00)	3.50 (2.00 – 5.00)	4.00 (2.00 – 4.05)
$t_{1/2}$[c] (h)	24.5 (17.0 – 52.2)	32.5 (25.1 – 45.4)	NC
CL/F (L/h)	33.6 (47)	NA	NA
V_z/F (L)	1190 (19)	NA	NA
V_{ss}/F (L)	1140 (28)	NA	NA

Note: Concentrations of total radioactivity in whole blood were not quantifiable for a sufficient duration to reliably determine AUC(0-∞). Instead, partial AUCs up to the last common quantifiable timepoint for all subjects in plasma and whole blood, AUC(0-48) and AUC(0-10), respectively, were used for calculation of ratios of plasma LY3202626 relative to plasma total radioactivity and ratios of whole blood to plasma total radioactivity.

a Data presented as ng equivalents/g, as applicable.

b Median (range).

c Geometric mean (range).

Table 2: Percent of sample radioactivity as [^{14}C]LY3202626 or metabolites of [^{14}C]LY3202626 in pooled human plasma samples after a single oral dose of 10 mg [^{14}C]LY3202626

Peak	[M+H]$^+$	Proposed Metabolite Identification	Percent of Radioactivity (% of Run)			
			4 hr	144 hr	288 hr	AUC pool (0-24hr)
Parent	499	LY3202626	43.4	8.96	1.63	38
M1	363	Amide hydrolysis to the amine (aniline) (LSN3200635)	1.28	17.2	24.3	2.27
M2	485	O-desmethyl (LSN3207841)	4.13	11.3	10.3	4.41
M3	155	Amide hydrolysis to the carboxylic acid (LSN3170994)	3.64	<1.0	<1.0	3.86
M4	212	M3 + glycine (LSN3329581)	10.3	1.57	<1.0	11.9
M5	405	N-acetyl of M1 (LSN3226305)	<0.5	<1.0	<1.0	<1.0
M16	460	M2 - O (reduction) (LSN3420637)	<1.0	2.1	1.81	<1.0
Region A			30.0	46.9	54.3	33.5
Total			92.76	88.03	92.24	93.94
Total radioactivity recovery			103.0	101.3	103.0	96.7

Table 3: Percent Dose of LY3202626 and its Metabolites Excreted in Urine and Feces from Healthy Human Subjects After a Single Oral Dose of 10 mg [^{14}C]LY3202626 from 0-508 hours

Peak	**$[M+H]^+$**	**Proposed Metabolite Identification**	**Percent of Dose**		
			Urine	**Feces**	**Total**
Parent	499	LY3202626	2.25	2.02	4.27
M1	363	Amide hydrolysis to the amine (aniline) (LSN3200635)	1.21	ND	1.21
M2	485	O-desmethyl (LSN3207841)	8.88	10.75	19.63
M4	212	M3 + glycine (LSN3329581)	21.27	ND	21.27
M5	405	N-acetyl of M1 (LSN3226305)	0.18	1.32	1.5
M16	460	M2 - O (reduction) (LSN3420637)	ND	6.94	6.94
M21	499	Same mass as parent	1.34	1.55	2.89
Total % Identified			35.15	22.57	57.72
Total % Dose in the Sample Analyzed			40.99	28.81	69.8

Table 4: Permeability in MDCK-MDR1 Monolayers for LSN3207841(M2) and LSN3420637 (M16) and LSN3182170 (HCl Salt of LY3202626, Parent)

Compound		rD0, µM	Pe ± SD ×10^{-6} cm/s	% cell ± SD	% recovery	Pe $_{BL/AP}$	Pe $_{c/I}$	P-gp	Pgp inhibition %		Comments
									5 µM	25 µM	
M2	**P-gp inhibited**							Yes	0	0	Very slow Pe, very low % cell, inhibition unlikely
	A-B	3.5	1.1±0.25	0.34±0.00	102±0.56	0.71	29				
	B-A	3.3	0.80±0.00	0.31±0.00	100±5.1						
	P-gp active										
	A-B	3.3	0.57±0.05	0.30±0.02	100±1.4	21					
	B-A	3.4	12±0.26	0.27±0.02	89±3.6						
M16	**P-gp inhibited**							Yes	1	21	Fast Pe, moderate % cell, inhibition unlikely
	A-B	3.5	53±0.14	20±0.18	154±0.40	0.99	6.1				
	B-A	2.8	53±0.04	19±0.73	130±3.9						
	P-gp active										
	A-B	2.6	16±2.1	11±0.09	115±5.7	6.0					
	B-A	2.6	97±0.62	7.9±0.42	125±4.1						
Parent	**P-gp Inhibited**							No	6	25	Fast Pe, high partitioning, inhibition unlikely
	A-B	2.1	19±2.3	50±0.53	92±8.6	1.2	1.5				
	B-A	2.4	21±0.02	28±0.00	97±5.5						
	P-gp active										
	A-B	2.8	15±0.13	49±1.6	88±0.25	1.8					
	B-A	2.7	27±1.1	27±5.4	94±1.4						

rD0: measured concentration of recovered donor solution at t=60 min

Pe: apparent permeability coefficient (n=2) with 60 min time interval: AB, BA>15, fast; AB, BA is 2-15, moderate; AB, BA is 1-2, slow; AB, BA is <1, very slow.

% Cell: amount extracted from cell with methanol relative to recovered mass: <1%, very low; 1-5%, low; 6-20%, moderate; 21-89%, high; ≥90%, very high (invalidates Pe values because compound prefers lipid environment, assay artifact).

%Recovery: mass of D60+cell60+R60/D0 (measured concentration of donor solution at t=0) x 100. If >100%, then D0 is underestimated.

Pe $_{BL/AP}$: ratio of Pe values in B to A and A to B directions; >3.0+active efflux.

Pe $_{C/I}$: Net efflux ratio=inhibited BA/AB and Control BA/AB ratio. Pgp Yes (Y) or No (N) or Unknown (U): If ≥3, Y; <3, N; If % Cell >90, U.

Pgp inhibition: two concentrations (5 and 25 µM) tested for Calcein-AM uptake assay in MDCK-MDR1 cells; % inhibition vs. LSN335984 (EC50=0.15-0.3 µM), pending at 5 uM: 0-20, inhibition unlikely, 21-50, partial inhibition possible, >51%, partial inhibition likely.

DMD Fast Forward. Published on June 4, 2020 as DOI: 10.1124/dmd.120.000009
This article has not been copyedited and formatted. The final version may differ from this version.

Figure 1

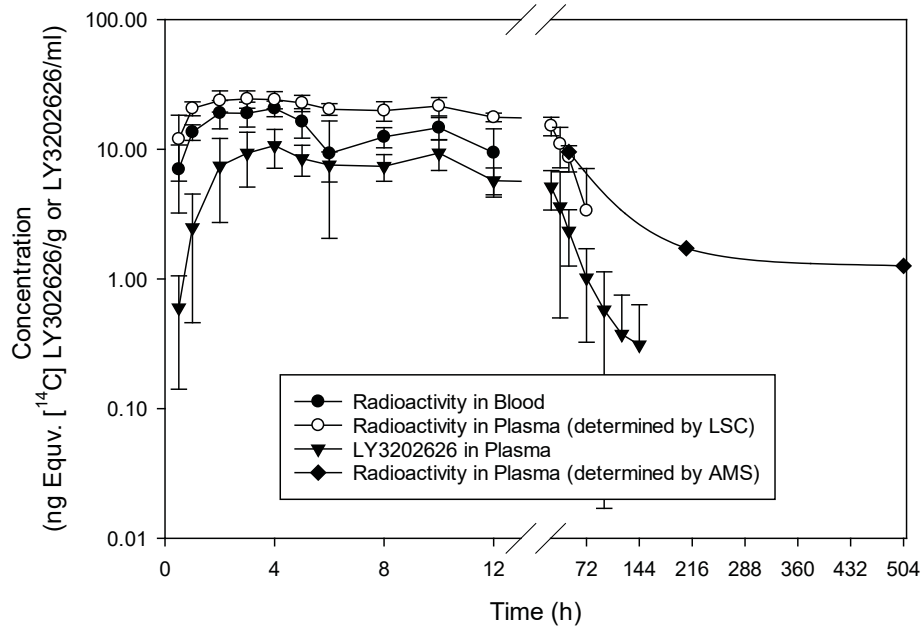

Figure 2

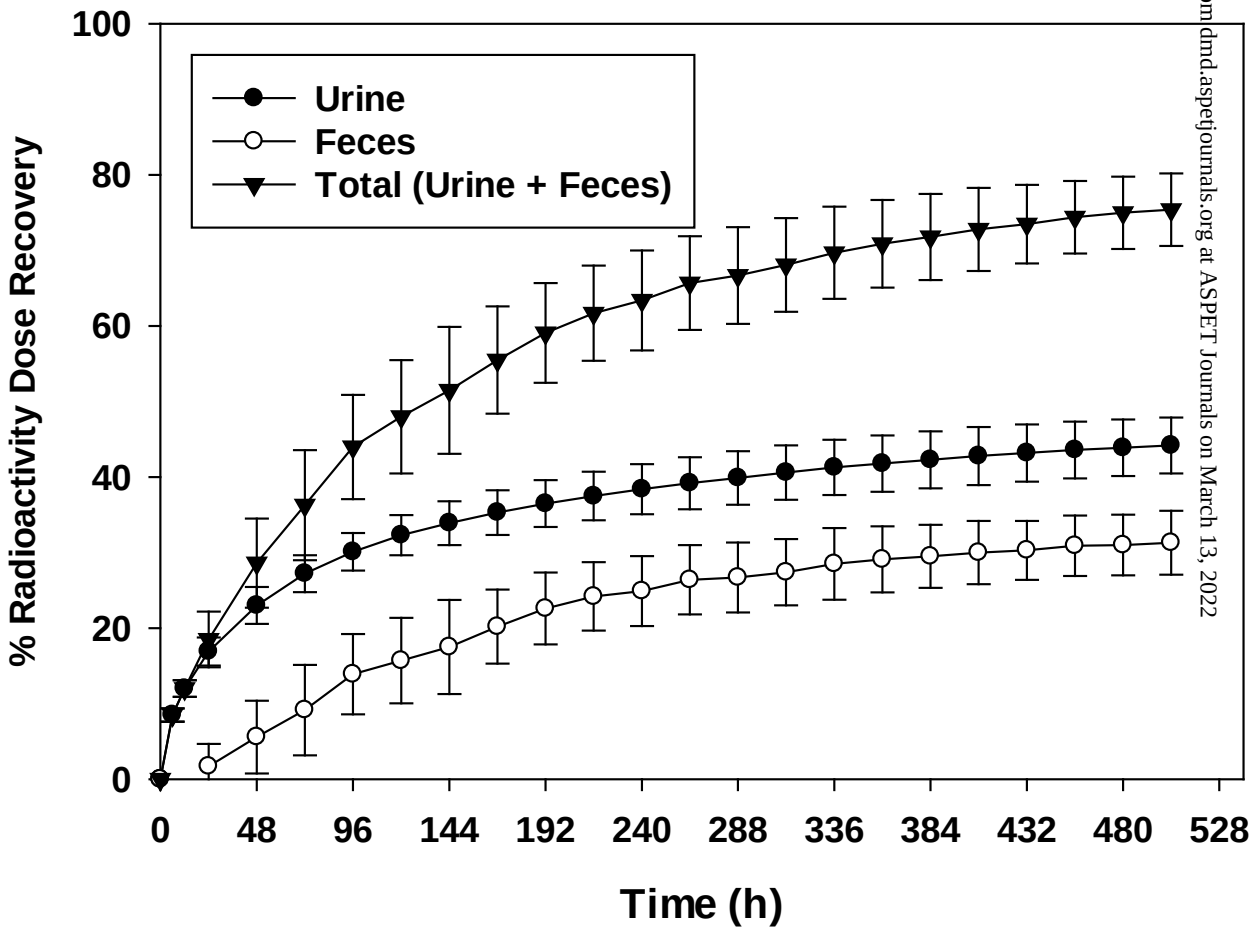

DMD Fast Forward. Published on June 4, 2020 as DOI: 10.1124/dmd.120.000009
This article has not been copyedited and formatted. The final version may differ from this version.

Figure 3

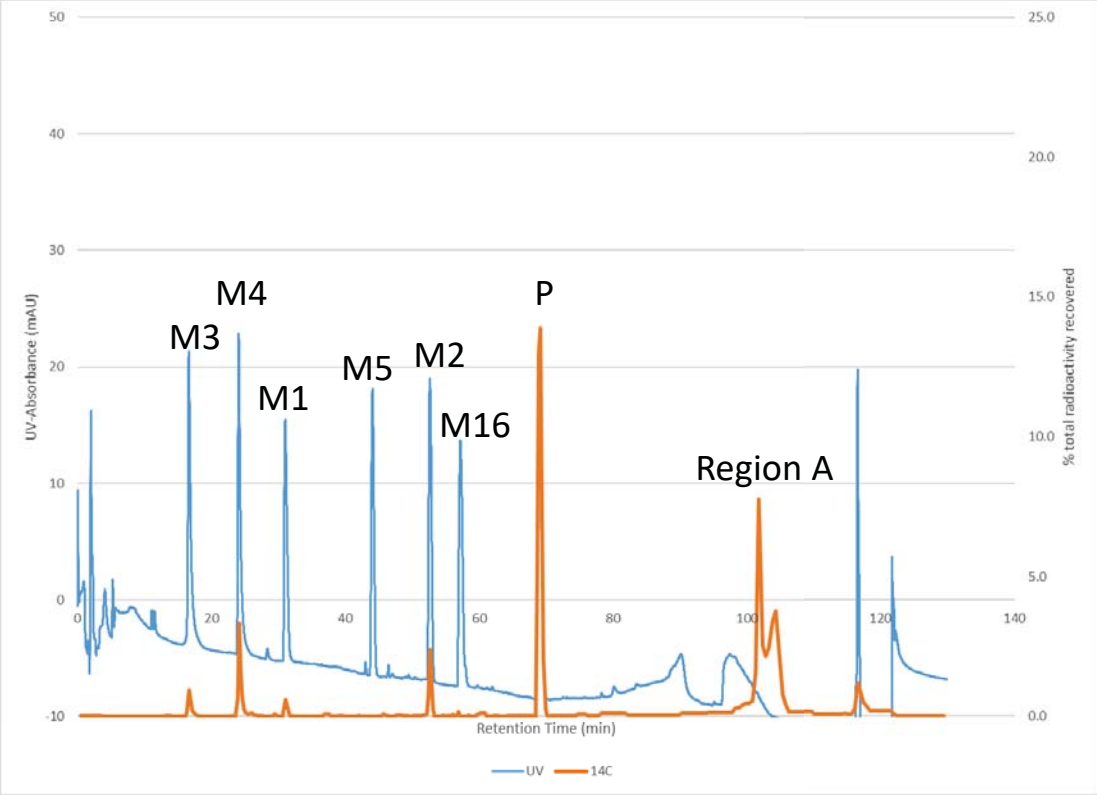

DMD Fast Forward. Published on June 4, 2020 as DOI: 10.1124/dmd.120.000009
This article has not been copyedited and formatted. The final version may differ from this version.

Figure 4

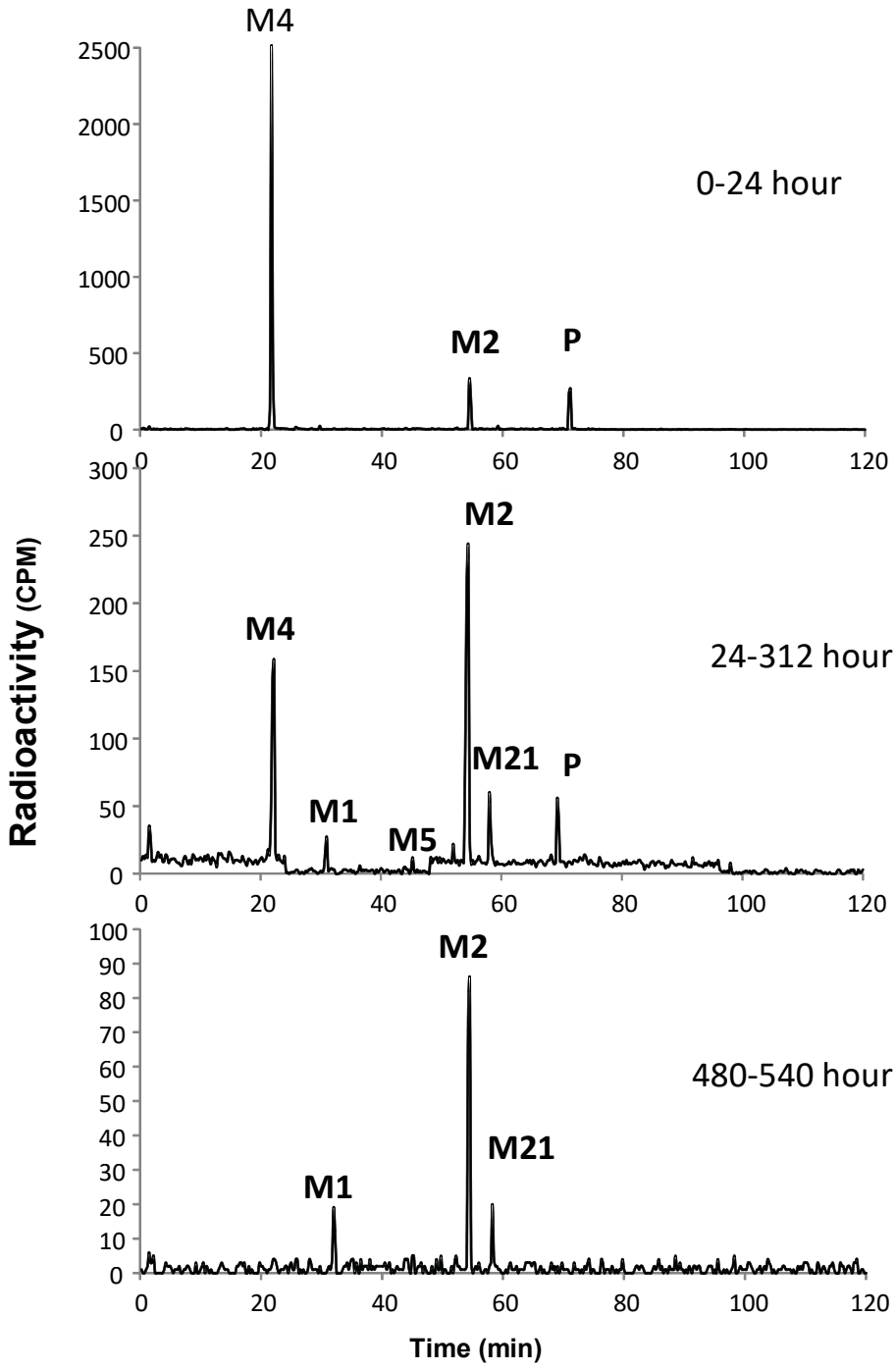

DMD Fast Forward. Published on June 4, 2020 as DOI: 10.1124/dmd.120.000009
This article has not been copyedited and formatted. The final version may differ from this version.

Figure 5

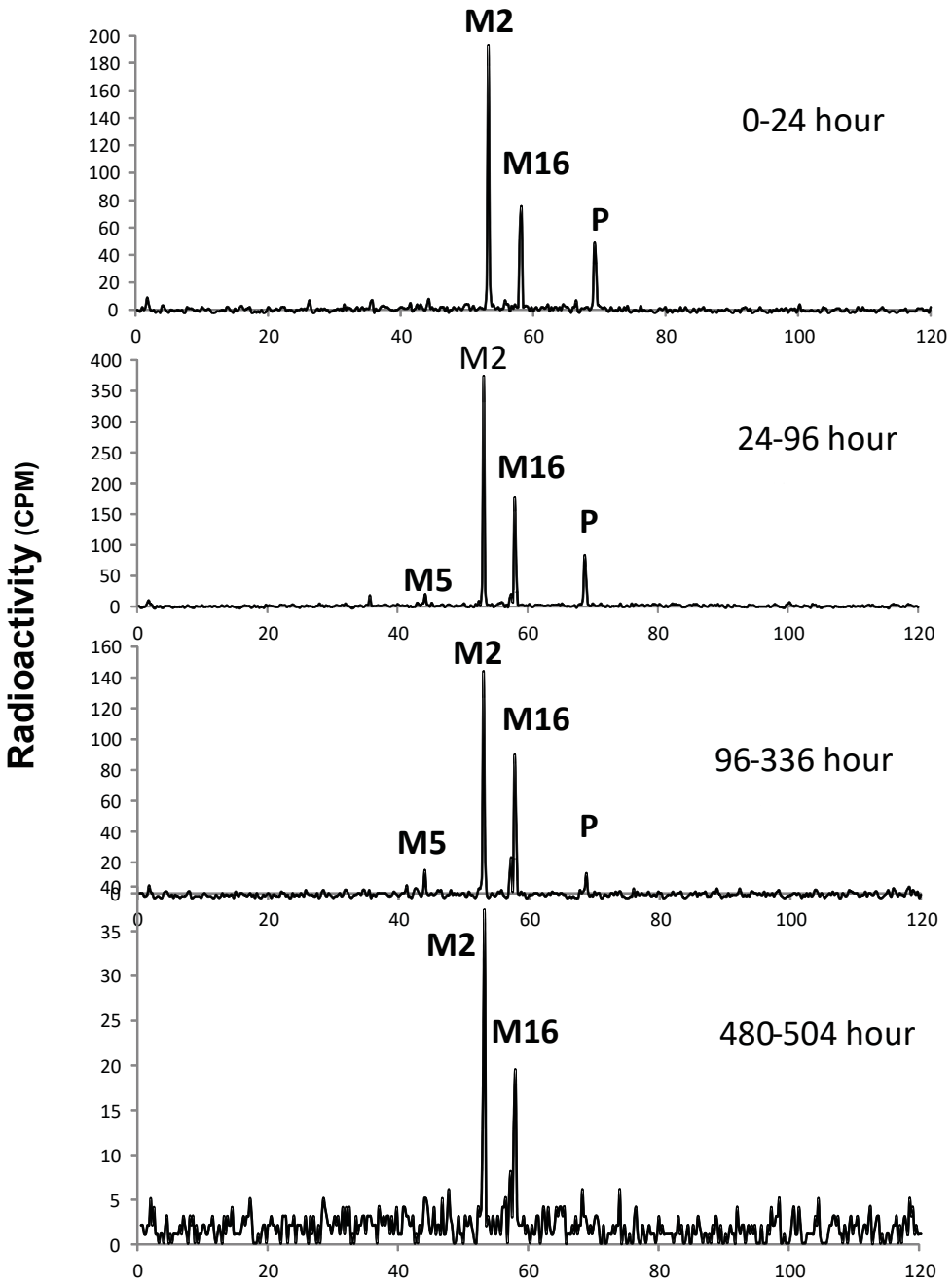

DMD Fast Forward. Published on June 4, 2020 as DOI: 10.1124/dmd.120.000009
This article has not been copyedited and formatted. The final version may differ from this version.

Figure 6A

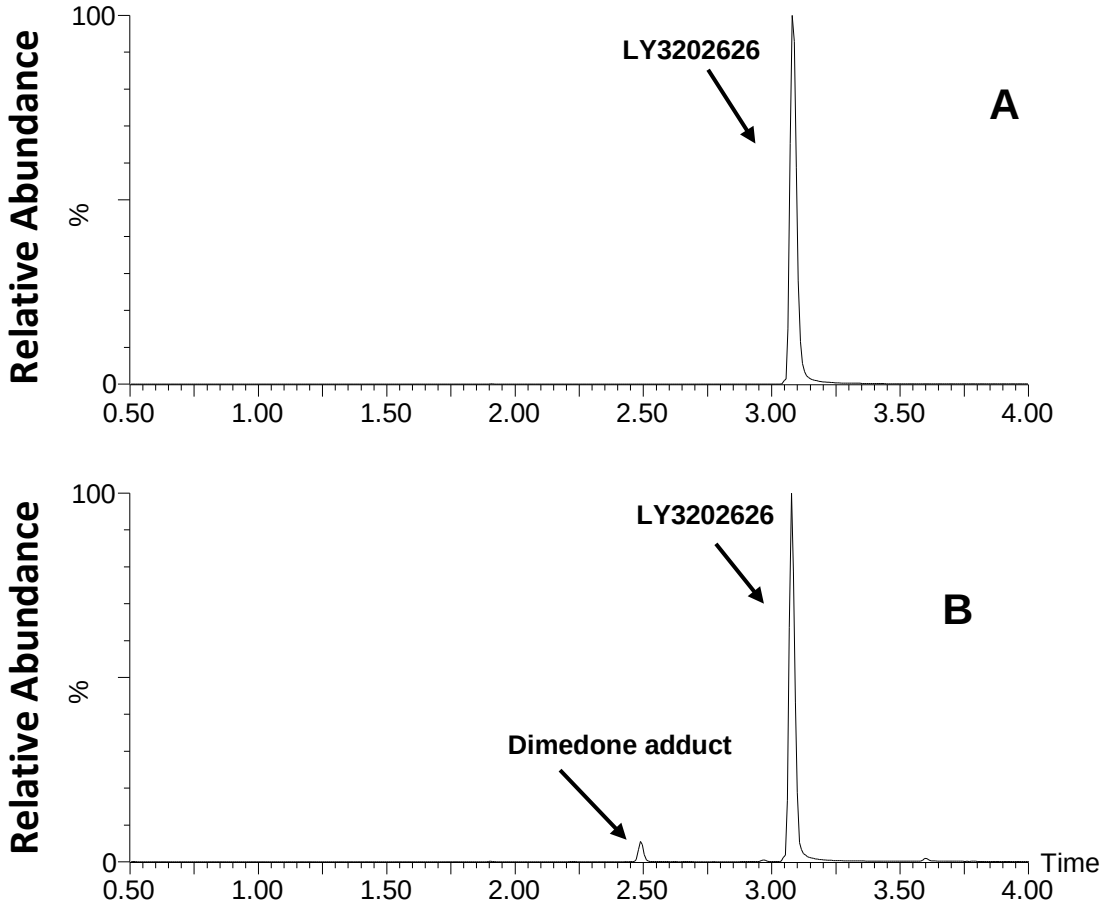

Figure 6B

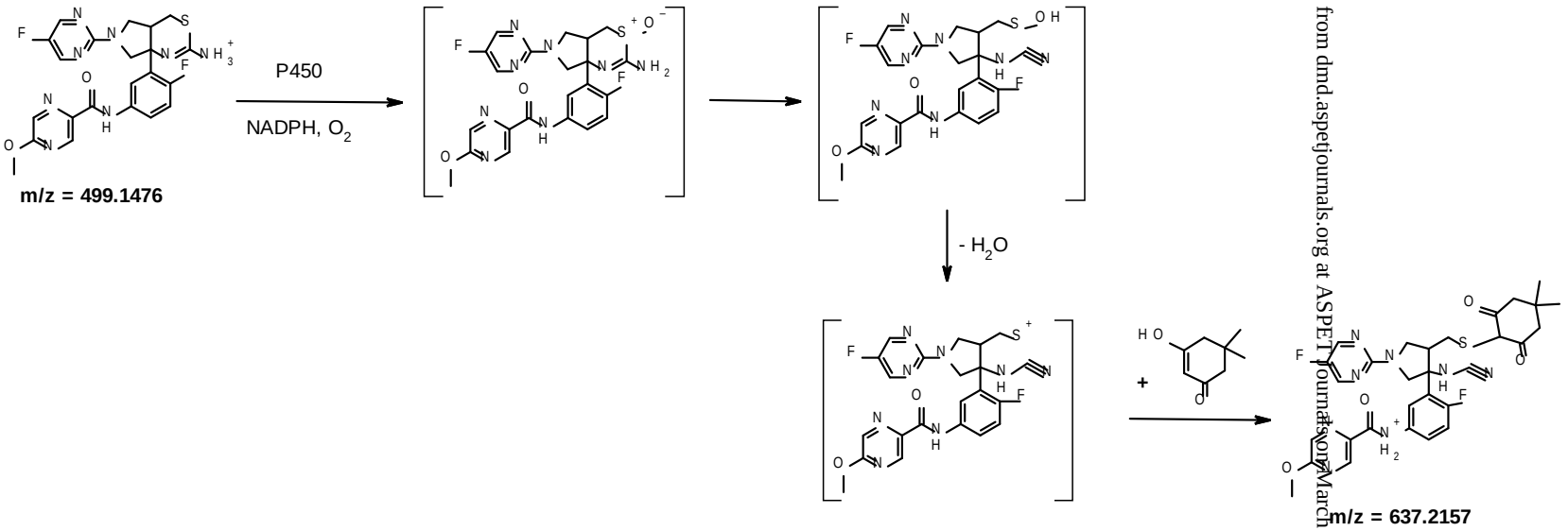

DMD Fast Forward. Published on June 4, 2020 as DOI: 10.1124/dmd.120.000009
This article has not been copyedited and formatted. The final version may differ from this version.

Figure 7

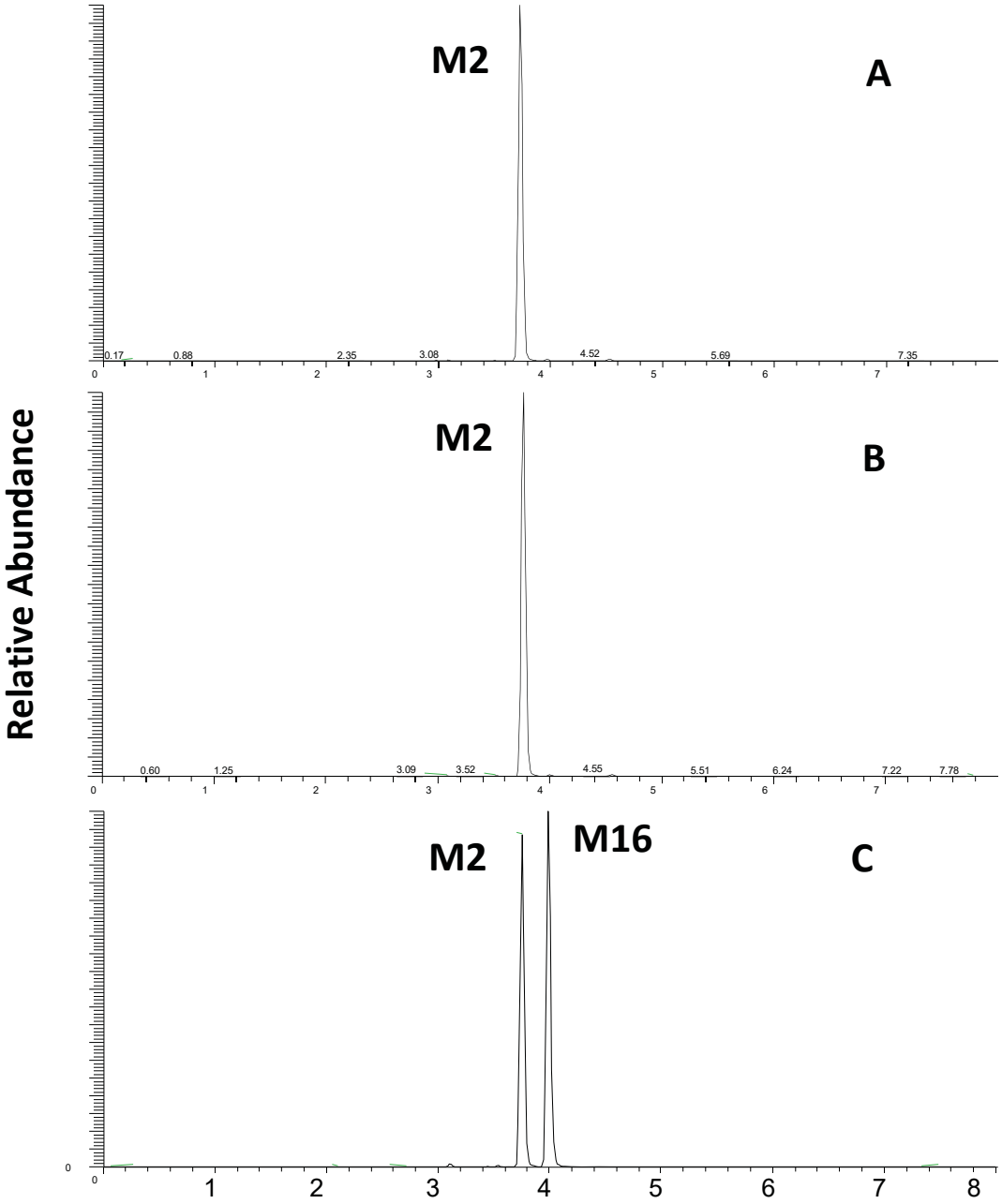

DMD Fast Forward. Published on June 4, 2020 as DOI: 10.1124/dmd.120.000009
This article has not been copyedited and formatted. The final version may differ from this version.

Figure 8

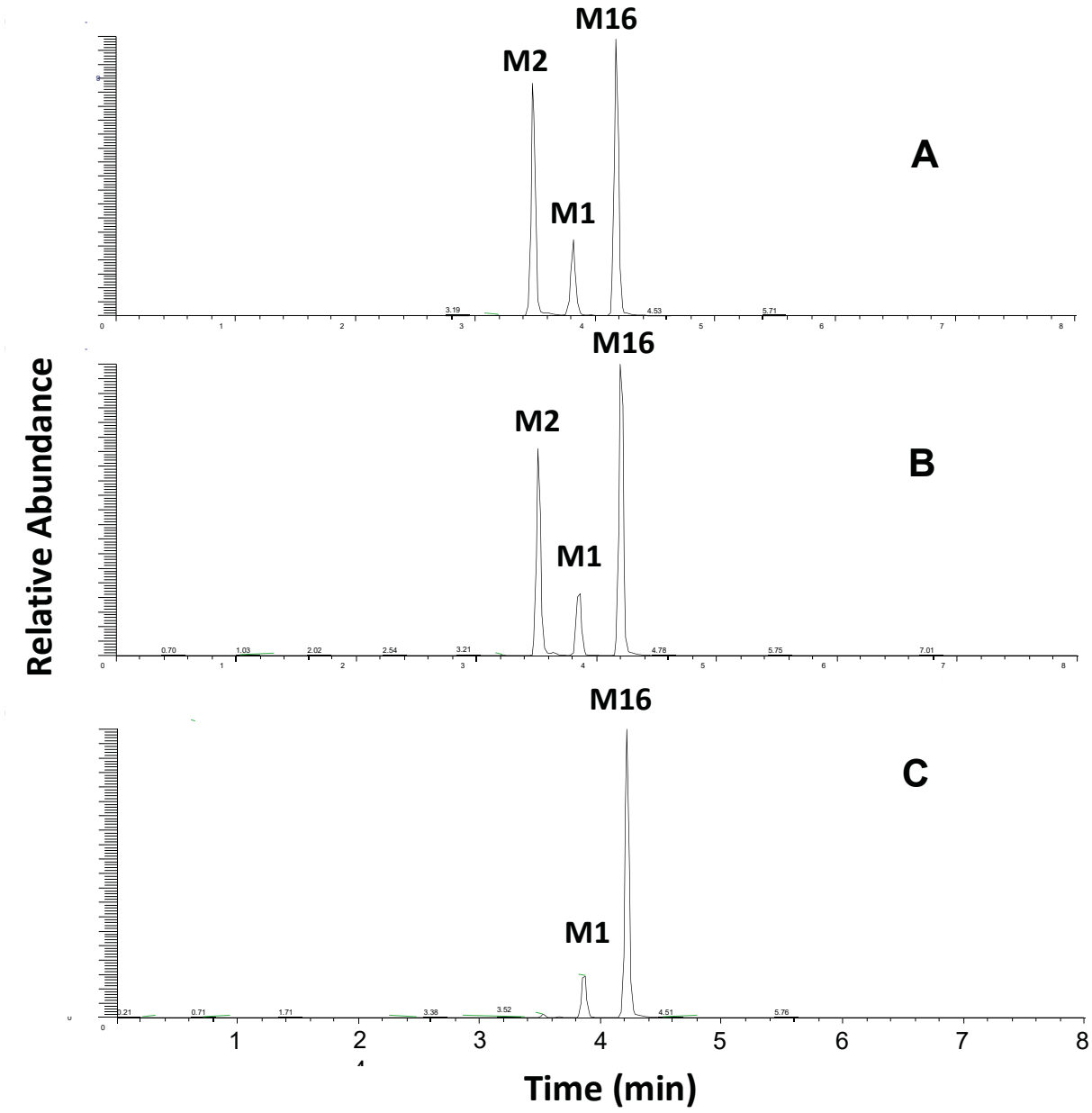

DMD Fast Forward. Published on June 4, 2020 as DOI: 10.1124/dmd.120.000009
This article has not been copyedited and formatted. The final version may differ from this version.

Figure 9

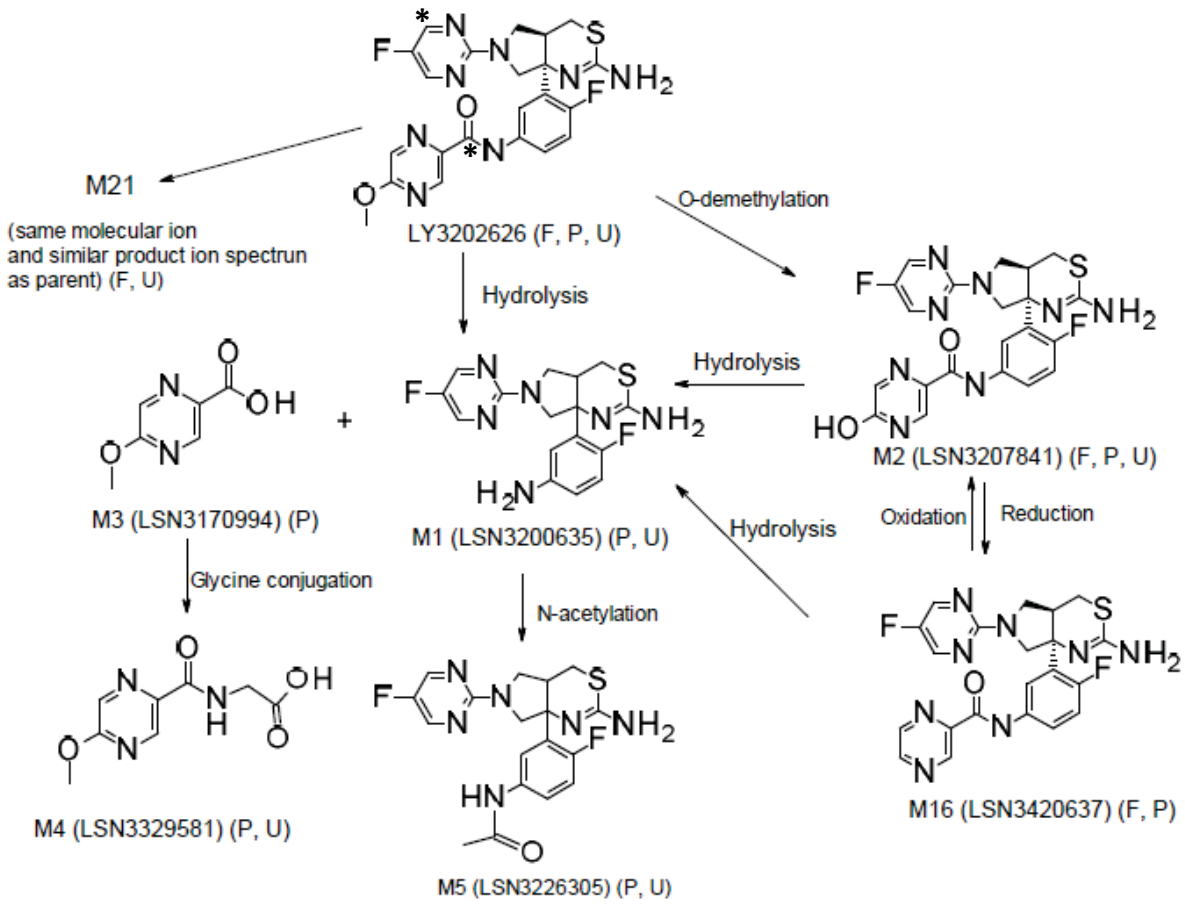

DMD Fast Forward. Published on June 4, 2020 as DOI: 10.1124/dmd.120.000009
This article has not been copyedited and formatted. The final version may differ from this version.

Figure 10